

Cluster formation in two-component Fermi gases

X. Y. Yin,¹ Hui Hu,¹ and Xia-Ji Liu¹

¹Centre for Quantum and Optical Science, Swinburne University of Technology, Melbourne, Victoria 3122, Australia

(Dated: July 29, 2019)

Two-component fermions are known to behave like a gas of molecules in the limit of Bose-Einstein condensation of diatomic pairs tightly bound with zero-range interactions. We discover that the formation of cluster states occurs when the effective range of two-body interaction exceeds roughly 0.46 times the scattering length, regardless of the details of the short-range interaction. Using explicitly correlated Gaussian basis set expansion approach, we calculate the binding energy of cluster states in trapped few-body systems and show the difference of structural properties between cluster states and gas-like states. We identify the condition for cluster formation and discuss potential observation of cluster states in experiments.

Introduction: A fermion is a particle that follows Fermi-Dirac statistics, which gives rise to Pauli exclusion principle [1]. The Pauli exclusion principle states that two or more identical fermions cannot occupy the same quantum state within a quantum system. The result is the emergence of Fermi pressure that prevents white dwarfs and neutron stars from gravitational collapse [2].

Fermi pressure is also responsible for stabilizing dilute two-component Fermi gases [3–6]. As the strength of two-body interaction changes, the two-component Fermi gases experience a crossover from weakly correlated Bardeen-Cooper-Schrieffer (BCS) pairing to a Bose-Einstein condensate (BEC) of tightly bound pairs [7, 8]. In the BEC limit of the BCS-BEC crossover, two unlike fermions form a molecule, which is a composite boson [3, 4]. The system is then governed by dimer-dimer interactions between molecules. Structureless bosons with two-body interactions are known to form cluster states, such as three-body Efimov states [9]. However, such cluster states have not yet been found in two-component Fermi gases in the BEC limit. Previous numerical calculations in few-body systems [10, 11] and larger systems [4, 12] focused on the zero-range limit and no cluster states were found. The reason is that the Fermi pressure between identical fermions prevents such cluster states to form. However, cluster states could in principle exist with finite-range interactions. In this Letter, we show that the formation of cluster states occurs when the effective range of the two-body interaction exceeds roughly 0.46 times the scattering length, regardless of the details of the short-range interaction.

The identification of such cluster states are crucial in three ways. First, the formation of clusters in small two-component Fermi gases in three dimension (3D) corresponds to a phase transition from a droplet-like phase to a gas-like phase in many-body systems. This is reminiscent of the Luttinger liquid and gas of molecule transition in one dimension [13]. Second, the condition for cluster formation is important for preparing such systems in the lab. The magnitude of effective range can approach that of the scattering length in the vicinity of a Feshbach res-

onance [14]. Current technology allows preparing Fermi gases interacting through large effective range [15, 16]. The stability of the system and the atom loss rate will be strongly affected by the cluster formation. Third, two-component Fermi gases share similarities with the low-density regions of a neutron star interior where the scaled interaction strength varies and the effective range is, in general, not negligible [17]. Therefore, the parameter regime in certain parts of the neutron star can overlap with our study. Our results can provide insights in stability of local regions inside a neutron star.

Previous studies discussed the instability of trapped fermionic gases with attractive interactions within the mean-field frame work and the range of interaction was identified as an important factor [5]. Here, we pursue an *ab initial* calculation using explicitly correlated Gaussian (ECG) basis set expansion approach to study small systems consisting up to 6 particles. The microscopic approach has been proven successful in understanding physics in larger systems [6, 18].

System Hamiltonian: We consider equal mass two-component Fermi gases in 3D consisting of N_\uparrow spin-up and N_\downarrow spin-down atoms ($N_\uparrow = N_\downarrow = N$) under external spherically symmetric harmonic confinement with angular trapping frequency ω . The system Hamiltonian H reads

$$H = \sum_{i_\uparrow=1}^N \left(-\frac{\hbar^2}{2m} \nabla_{i_\uparrow}^2 + \frac{1}{2} m \omega^2 \vec{r}_{i_\uparrow}^2 \right) + \sum_{i_\downarrow=1}^N \left(-\frac{\hbar^2}{2m} \nabla_{i_\downarrow}^2 + \frac{1}{2} m \omega^2 \vec{r}_{i_\downarrow}^2 \right) + \sum_{i_\uparrow=1}^N \sum_{i_\downarrow=1}^N V_{2b}(r_{i_\uparrow i_\downarrow}), \quad (1)$$

where m denotes the mass of a single atom, \vec{r}_{i_\uparrow} and \vec{r}_{i_\downarrow} denote the position vector of the i th spin-up and down atom with respect to the trap center, respectively. We define the harmonic oscillator length $a_{\text{ho}} = \sqrt{\hbar/(m\omega)}$ and harmonic oscillator energy $E_{\text{ho}} = \hbar\omega$. Interspecies two-body interaction potential V_{2b} depends on the interparticle distance $r_{i_\uparrow i_\downarrow}$, $r_{i_\uparrow i_\downarrow} = |\vec{r}_{i_\uparrow} - \vec{r}_{i_\downarrow}|$.

We consider three different short-range potentials: (i) an attractive Gaussian potential with a repulsive core,

$V_{2b}^{(i)}(r) = V_0 \exp(-r^2/4r_0^2) - 2V_0 \exp(-r^2/2r_0^2)$; (ii) an attractive Gaussian potential, $V_{2b}^{(ii)}(r) = V_0 \exp(-r^2/2r_0^2)$; and (iii) a modified attractive Gaussian potential, $V_{2b}^{(iii)}(r) = rV_0 \exp(-r^2/2r_0^2)$. The scattering phase shift of two particles at low energy can be expanded as $-k \cot[\delta(k)] = 1/a_s - r_{\text{eff}}k^2/2$, where k is the wave vector, a_s the s -wave scattering length, and r_{eff} the effective range. For a fixed r_0 , we adjust V_0 such that $V_{2b}(r)$ has a certain a_s . For all three types considered, shallow attractive potentials do not support two-body s -wave bound state in free-space. As the depth increases, the potential supports successively more two-body bound states [6]. In this work, we only consider attractive potentials that support one s -wave bound state in free space (see Supplemental Material [19]). We then calculate r_{eff} for such potential. Solid, dashed, and dotted lines in Fig. 1 show potentials (i), (ii), and (iii) that produce the same $a_s = 0.2a_{\text{ho}}$ and $r_{\text{eff}} = 0.09a_{\text{ho}}$, respectively. We will show later that the condition for cluster formation does not strongly depend on the type of potential. This indicates that the physics is well described by the two parameters a_s and r_{eff} alone. Although all three types are short-range, potential (i) simulates the repulsive core in realistic atom-atom interactions and can produce a larger range of r_{eff} for a fixed a_s .

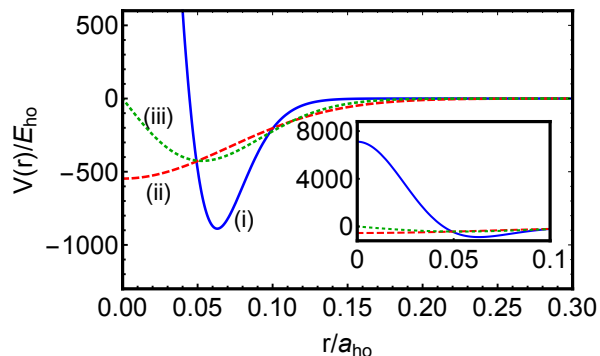


FIG. 1. (Color online) Solid, dashed, and dotted lines show the short range potential curves (i), (ii) and (iii), respectively. The value of a_s and r_{eff} coincides with the condition for cluster formation presented later in Fig. 4. Inset shows the same plot on a different scale.

We solve the time-independent Schrödinger equation for the Hamiltonian given in Eq. (1) using explicitly correlated Gaussian (ECG) basis set expansion approach [20]. After separating off the center-of-mass degrees of freedom, we expand the eigenstates of the relative Hamiltonian in terms of ECG basis functions, which depend on a number of nonlinear variational parameters that are optimized through energy minimization [10, 11, 20, 21].

Bound state energy: Trapped (1, 1) system, consisting one spin-up and one spin-down particle has been solved analytically. The exact energy spectrum for zero-range

interaction is given in Ref. [22] while the contribution from the effective range is discussed in Ref. [23]. When a_s is positive and much smaller than a_{ho} , the binding energy of the two-particle pair with short-range interaction can be approximated by $E_s = -\hbar^2/(ma_s^2)$. For $a_s = 0.2a_{\text{ho}}$, the binding energy is approximately $-25E_{\text{ho}}$ and decreases with increasing r_{eff} .

For trapped two-component Fermi gases with more particles, i.e., (N, N) systems, two particles with opposite spin form a molecule just like in (1, 1) system. Such molecules were often treated as composite bosons and an effective model with effective dimer-dimer interactions are shown to be very accurate in the zero-range limit [3, 10, 11]. In this effective model, the dimer-dimer interaction has a scattering length $a_{dd} = 0.608a_s$, a small positive value compared to a_{ho} , and does not support any bound state of two dimers [3]. This indicates that a dilute two-component Fermi gas behaves like a Bose gas with hard-core repulsion in the BEC and zero-range limit. However, dimer-dimer interaction is not *a priori* repulsive and cluster states can in principle exist. An important question is what is the condition for clusters to form. In the following, we will show that the effective range r_{eff} plays an important role.

We calculate the relative ground state energies of (1, 1), (2, 2), and (3, 3) systems, E_{11} , E_{22} , and E_{33} , respectively, for fixed $a_s = 0.2a_{\text{ho}}$ and a wide range of r_{eff} . The center-of-mass energy is simply $3\hbar\omega/2$ for all systems and is not included in our results. To identify the cluster formation between dimers, we follow Ref. [10] and subtract the energy of molecules from the four- and six-body systems, i.e., we plot $\Delta E_{22} = E_{22} - 2E_{11}$ and $\Delta E_{33} = E_{33} - 3E_{11}$ as a function of r_{eff} in Fig. 2. Circles, squares, and diamonds are for potential (i), (ii), and (iii), respectively. For small r_{eff} , our results agree with previous studies: ΔE_{22} and ΔE_{33} are positive, and agree with the zero-range ground state energy for two and three weakly repulsive bosons with dimer-dimer scattering length $a_{dd} = 0.608a_s$, which are marked as dotted lines in the insets. This indicates that the ground state is indeed a gas-like state. Energies ΔE_{22} and ΔE_{33} remain largely unchanged as r_{eff} increases. As r_{eff} approaches $0.09a_{\text{ho}}$, ΔE_{22} and ΔE_{33} decrease suddenly and turn negative for all three types of interactions, signalling the formation of bound states between dimers. Note that the magnitude of ΔE_{33} is several times larger than ΔE_{22} , indicating that the bound state in (3, 3) system is indeed a three-dimer bound state, instead of a two-dimer bound state plus a single dimer. Our calculations show that r_{eff} at which cluster starts to form is largely independent of the details of the two-body interactions and is roughly the same for (2,2) and (3,3) systems. This shows that r_{eff} is the deciding factor for cluster formation in two-component Fermi gases.

Our physics picture is as follows. The existence of cluster states in two-component Fermi gases is deter-

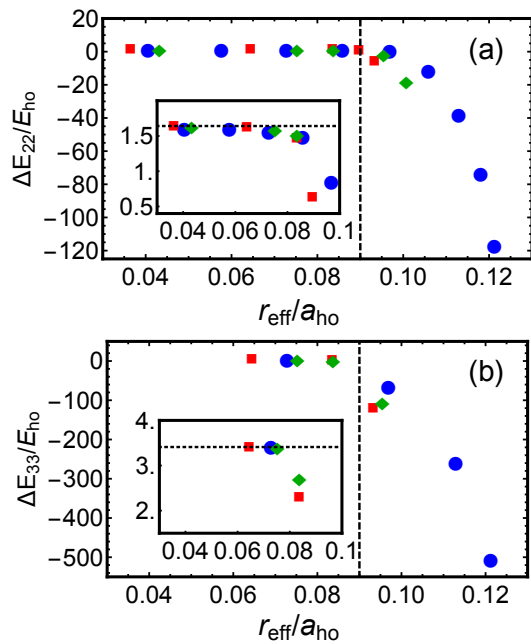


FIG. 2. (Color online) Panel (a) and (b) show the relative ground state energy for (2,2) and (3,3) systems subtracting the dimer energies, $\Delta E_{22} = E_{22} - 2E_{11}$ and $\Delta E_{33} = E_{33} - 3E_{11}$, as a function of effective range r_{eff} for $a_s = 0.2a_{\text{ho}}$. Blue circles, red squares, and green diamonds are calculated from potential (i), (ii), and (iii), respectively. Dashed vertical line $r_{\text{eff}} = 0.09a_{\text{ho}}$ marks the value of r_{eff} where clusters start to form. Insets show a magnified region with positive energy. Horizontal dotted line marks the energies calculated from effective dimer model.

mined by the counterbalance between the Fermi pressure between like-particles and the dimer-dimer interaction. The Fermi pressure is a short-range effect, preventing like fermions from getting close to each other through the requirement of anti-symmetrization. On the other hand, cluster formation requires all particles, like or unlike, to be at distances of the order of r_{eff} [3]. When r_{eff} is small, the anti-symmetrization of two like fermions cannot happen within such small distance. Therefore, such interaction cannot support bound states between dimers. When r_{eff} becomes larger, the dimer-dimer interaction can potentially overcome the Fermi pressure, allowing anti-symmetrization of two like fermions to happen within the range of r_{eff} .

Structural properties: In order to take a peak at the wave function, we calculate several structural properties for both gas-like and cluster states interacting through potential (i). First, we consider the spherically symmetric radial density $P_1(r)$, which tells the likelihood of finding a particle at distance r from trap center, with normalization $4\pi \int_0^\infty P_1(r)r^2 dr = 1$. Figure 3(a) and (d) show the radial density $P_1(r)$ for gas-like and cluster state, respectively. For both states, $P_1(r)$ peaks at the trap center and decays towards the edge. The overall extent

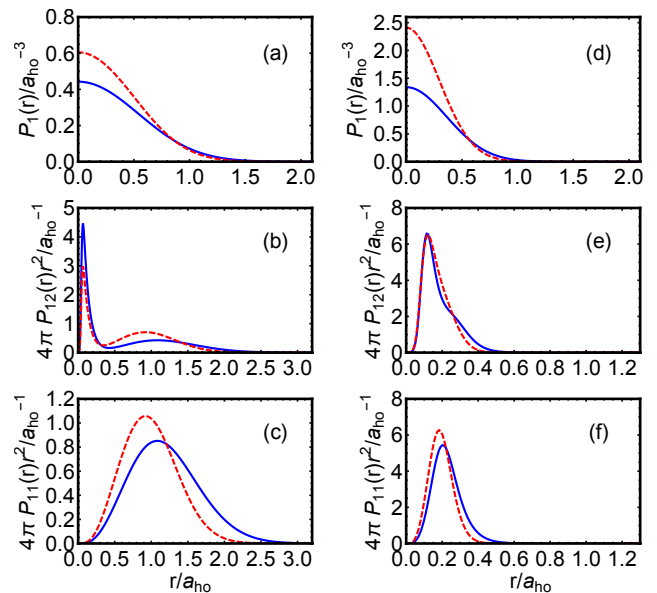


FIG. 3. (Color online) Solid and dashed lines show the structural properties for (2,2) and (3,3) systems, respectively. (a), (b), and (c) show the radial density $P_1(r)$, scaled distribution function between unlike pair $4\pi P_{12}(r)r^2$, and like pair $4\pi P_{11}(r)r^2$ for gas-like state with $a_s = 0.2a_{\text{ho}}$ and $r_{\text{eff}} = 0.073a_{\text{ho}}$. (e), (f), and (g) show the same quantities as in (a), (b), and (c), but for cluster state with $a_s = 0.2a_{\text{ho}}$ and $r_{\text{eff}} = 0.113a_{\text{ho}}$.

of a single particle can be measured by expectation value $\langle r \rangle = 4\pi \int_0^\infty P_1(r)r^3 dr$. For both (2,2) and (3,3) systems, the expectation values for the cluster states are about 30% lower than gas-like states (see Supplemental Material [19]). We confirm that the expectation values do not differ much for different r_{eff} within the gas-like state and cluster state. The drop in $\langle r \rangle$ represents a sudden change from gas-like to cluster state.

Second, we consider the scaled distribution function between unlike pair $4\pi P_{12}(r)r^2$, which tells the likelihood of finding two unlike particles at distance r from each other, with normalization $4\pi \int_0^\infty P_{12}(r)r^2 dr = 1$. Since we consider the BEC limit, it is natural to expect a sharp peak at a short distance that is of the order of a_s as two unlike particles form a molecule. Indeed, for both the gas-like and cluster states, a sharp peak at short distance is identified. A difference is that the distribution function for cluster state vanishes at the order of trap length a_{ho} while exhibits a lower and wider second peak for the gas-like state, which corresponds to the distribution between two unlike particles that belongs to different dimers.

Third, we consider the scaled distribution function between like pair $4\pi P_{11}(r)r^2$, which tells the likelihood of finding two like particles at distance r from each other with normalization $4\pi \int_0^\infty P_{11}(r)r^2 dr = 1$. The distribution function between like pair is a good gauge of the overall extent of the system. For gas-like state, a broad distribution centred around the trap length a_{ho} is ob-

served, confirming that the system is indeed extended to the confinement of the trap. For cluster state, we find that a peak appears at a similar distance to the unlike pair, which is an order of magnitude smaller than gas-like state. This difference clearly distinguishes the two states. Further details on the expectation values of distances between unlike and like pairs are discussed in Supplemental Material [19].

Condition for cluster formation: For a certain a_s , both the ground state energies and the structural properties exhibit a clear transition between the gas-like and cluster state that is driven by the effective range r_{eff} . For each a_s , boundary is determined through the sudden drop of ΔE_{22} [see, e.g., the rightmost red square in the inset of Fig. 2(a)]. We then analyze ΔE_{33} and the expectation values from structural properties [19] and find no discrepancy. This allows us to map out the condition for cluster formation in Fig. 4.

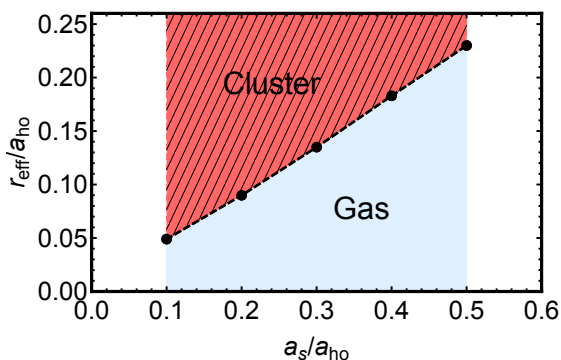


FIG. 4. (Color online) Boundary between the gas-like and cluster state in the parameter space of scattering length a_s and effective range r_{eff} . Hatched and solid regions correspond to the cluster state and gas-like state, respectively.

We make three observations. First, the boundary between the two classes can be approximated by a linear relation $r_{\text{eff}} = 0.46a_s$. A shorter range interaction produces a hard-core repulsive dimer-dimer interaction and results in a gas-like state. A longer range interaction, in contrast, can overcome the Fermi pressure and leads to cluster formation. Second, although we are not able to perform calculations for smaller a_s or r_{eff} due to numerical limitation, if we assume that the linear relation continues to smaller a_s , a vertical line $r_{\text{eff}} = 0$ will fall entirely into the gas-like state. This suggests that cluster states are absent for the zero-range interaction and confirms the conclusion in Ref. [4, 10–12]. Third, as we increase a_s , the region of cluster state shrinks. This indicates that it could be more difficult to find cluster states as the system moves towards the unitarity limit, i.e., with infinitely large scattering length. This could explain the observation in Ref. [24] where no cluster state was found for a wide range of r_{eff} .

Although we considered trapped few-body systems in

this work, we expect many of our findings to apply to larger and homogeneous systems (see Supplemental Material [19]). We also note that the transition between the gas-like and cluster state happens within very small parameter range, and the changes in ground state energy and structural properties are drastic. In the many-body limit, the transition could possibly correspond to a first-order phase transition to a phase-separation phase [25, 26].

Implications for experiments: Two-component Fermi gases in the BEC limit have been prepared in different cold atom systems. For example, a mixture of two hyperfine states, $|f, m_f\rangle = |9/2, -9/2\rangle$ and $|9/2, -5/2\rangle$, of ^{40}K have been prepared across the BEC-BCS crossover [27]. Other hyperfine states of ^{40}K [28] and other species such as ^6Li [29] have also been studied.

We consider neutral atom interactions modelled by van der Waals potential $V_{2b,\text{vdW}}(r_{ij}) = -C_6/r_{ij}^6$. The relation between r_{eff} and a_s was found to be $r_{\text{eff}} = \Gamma(1/4)^4 / (6\pi^2) \bar{a} [1 - 2\bar{a}/a_s + 2(\bar{a}/a_s)^2]$ [30] and shown to work reasonably well near broad Feshbach resonances [31]. Here, $\bar{a} = [4\pi/\Gamma(1/4)^2]R_{\text{vdW}}$, $R_{\text{vdW}} = (mC_6/\hbar^2)^{1/4}/2$, and $\Gamma(x)$ is the Gamma function. In the case of ^{40}K , R_{vdW} was calculated to be $64.90a_0$, where a_0 denotes the Bohr radius [32]. The scattering length is tunable near a Feshbach resonance between $|f, m_f\rangle = |9/2, -9/2\rangle$ and $|9/2, -5/2\rangle$, which is centred at $B_{\text{pk}} = 224.21\text{G}$ [27]. We therefore determine that the system is in gas-like state for magnetic field $200.3\text{G} < B < 233.9\text{G}$ (see Supplemental Material [19]). Within this range, the two-component Fermi gas went through the BEC-BCS crossover as observed in the experiments [27]. We expect cluster to form outside this range. This is consistent with the observations that two-component Fermi gases are generally stable near Feshbach resonances [3].

Cluster formation can potentially be observed through rf spectroscopy in a magnetically trapped two-component Fermi gas with thousands of atoms [27, 28]. Previous experimental measurements [27] on ^{40}K are performed with $215\text{G} < B < 230\text{G}$, which lies entirely within the gas-like state according to our prediction. Our results suggest that cluster formation may be observed further away from the Feshbach resonance. A more direct reproduction of the system we studied, i.e., a trapped system with only few atoms, can potentially be realized in optical tweezers [33, 34] and optical microtraps [35].

Final remarks: We studied the formation of cluster state in two-component Fermi gases by numerically calculating the ground state energy of a trapped few-body system interacting through various types of short-range potentials. Our findings corroborate the picture that the counterbalance between the Fermi pressure and the short-range interactions determines the boundary between the gas-like and cluster state. Although our calcu-

lations are performed with short-range interactions due to numerical restrictions, we expect such result to apply to realistic interactions because of the short-range nature of Fermi pressure. We also provide an estimate for the parameter regime where such cluster states could potentially be identified in the experiments.

We are grateful for discussions with Jia Wang and Yangqian Yan. This research was supported by the Australian Research Council (ARC) Discovery Programs, Grants No. DP170104008 (H.H.), No. FT140100003 and No. DP180102018 (X.-J.L).

-
- [1] E. Fermi, *Nuovo Cimento* **11**, 157 (1934).
 - [2] D. Koester and G. Chanmugam, *Reports on Progress in Physics* **53**, 837 (1990).
 - [3] D. S. Petrov, C. Salomon, and G. V. Shlyapnikov, *Phys. Rev. Lett.* **93**, 090404 (2004).
 - [4] G. E. Astrakharchik, J. Boronat, J. Casulleras, and S. Giorgini, *Phys. Rev. Lett.* **93**, 200404 (2004).
 - [5] B. M. Fregoso and G. Baym, *Phys. Rev. A* **73**, 043616 (2006).
 - [6] D. Blume, *Reports on Progress in Physics* **75**, 046401 (2012).
 - [7] C. A. Regal, M. Greiner, and D. S. Jin, *Phys. Rev. Lett.* **92**, 040403 (2004).
 - [8] M. W. Zwierlein, C. A. Stan, C. H. Schunck, S. M. F. Raupach, A. J. Kerman, and W. Ketterle, *Phys. Rev. Lett.* **92**, 120403 (2004).
 - [9] C. H. Greene, P. Giannakeas, and J. Pérez-Ríos, *Rev. Mod. Phys.* **89**, 035006 (2017).
 - [10] D. Blume and K. M. Daily, *Phys. Rev. A* **80**, 053626 (2009).
 - [11] D. Blume and K. M. Daily, *Comptes Rendus Physique* **12**, 86 (2011).
 - [12] D. Blume, J. von Stecher, and C. H. Greene, *Phys. Rev. Lett.* **99**, 233201 (2007).
 - [13] K. T. Law and D. E. Feldman, *Phys. Rev. Lett.* **101**, 096401 (2008).
 - [14] P. Dyke, S. E. Pollack, and R. G. Hulet, *Phys. Rev. A* **88**, 023625 (2013).
 - [15] C. Chin, R. Grimm, P. Julienne, and E. Tiesinga, *Rev. Mod. Phys.* **82**, 1225 (2010).
 - [16] E. L. Hazlett, Y. Zhang, R. W. Stites, and K. M. O'Hara, *Phys. Rev. Lett.* **108**, 045304 (2012).
 - [17] P. van Wyk, H. Tajima, D. Inotani, A. Ohnishi, and Y. Ohashi, *Phys. Rev. A* **97**, 013601 (2018).
 - [18] J. Levinsen, P. Massignan, S. Endo, and M. M. Parish, *Journal of Physics B: Atomic, Molecular and Optical Physics* **50**, 072001 (2017).
 - [19] See Supplemental Material at *insert link* for more details.
 - [20] J. Mitroy, S. Bubin, W. Horiuchi, Y. Suzuki, L. Adamowicz, W. Cencek, K. Szalewicz, J. Komasa, D. Blume, and K. Varga, *Rev. Mod. Phys.* **85**, 693 (2013).
 - [21] X. Y. Yin and D. Blume, *Phys. Rev. A* **92**, 013608 (2015).
 - [22] T. Busch, B.-G. Englert, K. Rzaewski, and M. Wilkens, *Found. of Phys.* **28**, 549 (1998).
 - [23] F. Werner and Y. Castin, *Phys. Rev. A* **86**, 013626 (2012).
 - [24] M. M. Forbes, S. Gandolfi, and A. Gezerlis, *Phys. Rev. A* **86**, 053603 (2012).
 - [25] S. Piatecki and W. Krauth, *Nature Communications* **5**, 3503 (2014).
 - [26] M. Berciu, *Phys. Rev. Lett.* **107**, 246403 (2011).
 - [27] C. A. Regal and D. S. Jin, *Phys. Rev. Lett.* **90**, 230404 (2003).
 - [28] C. A. Regal, M. Greiner, and D. S. Jin, *Phys. Rev. Lett.* **92**, 083201 (2004).
 - [29] M. Bartenstein, A. Altmeyer, S. Riedl, R. Geursen, S. Jochim, C. Chin, J. H. Denschlag, R. Grimm, A. Simoni, E. Tiesinga, C. J. Williams, and P. S. Julienne, *Phys. Rev. Lett.* **94**, 103201 (2005).
 - [30] B. Gao, *Phys. Rev. A* **58**, 1728 (1998).
 - [31] C. L. Blackley, P. S. Julienne, and J. M. Hutson, *Phys. Rev. A* **89**, 042701 (2014).
 - [32] A. Derevianko, W. R. Johnson, M. S. Safronova, and J. F. Babb, *Phys. Rev. Lett.* **82**, 3589 (1999).
 - [33] A. M. Kaufman, B. J. Lester, and C. A. Regal, *Phys. Rev. X* **2**, 041014 (2012).
 - [34] L. R. Liu, J. D. Hood, Y. Yu, J. T. Zhang, N. R. Hutzler, T. Rosenband, and K.-K. Ni, *Science* **360**, 900 (2018).
 - [35] F. Serwane, G. Zürn, T. Lompe, T. B. Ottenstein, A. N. Wenz, and S. Jochim, *Science* **332**, 336 (2011).

Supplemental Material for “Cluster formation in two-component Fermi gases”

X. Y. Yin,¹ Hui Hu,¹ and Xia-Ji Liu¹

¹Centre for Quantum and Optical Science, Swinburne University of Technology, Melbourne, Victoria 3122, Australia

DEEPER BOUND STATES SUPPORTED BY MODEL POTENTIALS

In this work, we only consider attractive potentials (i), (ii), and (iii) that support one s -wave bound state in free space. Here, we explain the reasoning for this consideration and discuss the relevance of deeper bound states supported by these potentials.

When these attractive potentials support only one s -wave bound state, the bound state is fairly universal, i.e., the binding energy depends mostly on a_s and r_{eff} . For example, the relative energies for trapped (1, 1) system with $a_s = 0.2a_{\text{ho}}$ and $r_{\text{eff}} = 0.06a_{\text{ho}}$ interacting with potentials (i), (ii), and (iii) are $-37.24E_{\text{ho}}$, $-37.45E_{\text{ho}}$, and $-37.35E_{\text{ho}}$, respectively, which differ by at most 0.6%.

When these potentials becomes deeper, they support successively more two-body bound states. These deeper bound states have much lower energies and their energies depend highly on the details of the potentials other than a_s and r_{eff} . In other words, the properties of these deeper bound states are highly non-universal. We consider again trapped (1, 1) system with $a_s = 0.2a_{\text{ho}}$ and $r_{\text{eff}} = 0.06a_{\text{ho}}$ interacting with potentials (i), (ii), and (iii) that support exactly two s -wave bound states in free space. The relative energies for the ground states are $-24589.2E_{\text{ho}}$, $-8495.09E_{\text{ho}}$, and $-8891.35E_{\text{ho}}$, respectively. As we can see, the ground state energies are vastly different, especially for potential (i). This is expected since the repulsive barrier can have a large impact on non-universal properties.

We also note that when the potentials support two bound states, the absolute value of binding energy of the ground state is 200 – 600 times higher than the first excited state. If realistic interactions in the experiments support more than one bound state, we expect them to be well separated in the relevant parameter regime. Hence, the deeper bound states should not play a significant role on the experimentally relevant time scale.

Since the deeper bound states are highly non-universal, the properties of two-component Fermi gases with more particles cannot be described by the framework in Ref. [1]. Naturally, our condition for cluster formation, which depends only on a_s and r_{eff} , also do not apply to these states.

CHEMICAL POTENTIAL FOR CLUSTER STATES

In this work, we consider (1, 1), (2, 2), and (3, 3) systems. To provide further insights into larger systems, we calculate the chemical potential. The chemical potential for few-body systems is defined as the energy change when adding one particle. For two-component Fermi gases, we consider $\mu = \mu_{\uparrow} + \mu_{\downarrow}$, that is the energy change when adding a two-particle pair. Specifically, we show $\mu_{11} = E_{22} - E_{11}$ and $\mu_{22} = E_{33} - E_{22}$ in Fig. S1. We additionally plotted E_{11} , which corresponds to the energy change when adding a pair to the vacuum.

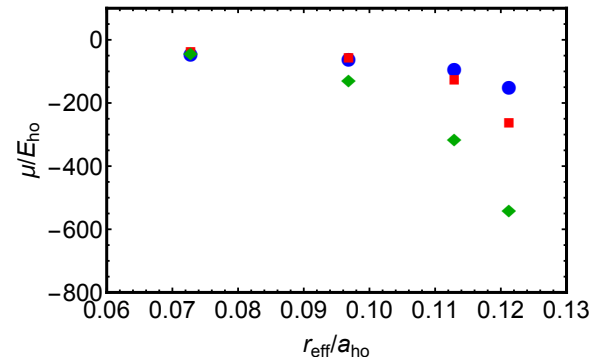


FIG. S1. (Color online) Blue circles, red squares, and green diamonds show the relative ground state energy of (1, 1) system E_{11} , chemical potential of (1, 1) system μ_{11} , and chemical potential of (2, 2) system μ_{22} , respectively. Calculations are done for type (i) potential with $a_s = 0.2a_{\text{ho}}$.

For gas-like state, the chemical potential remains a constant when number of particles increases. This constant is approximately equal to the energy of a dimer. For cluster state, we find that the absolute value of chemical potential increases with number of particles for the few-body systems that we considered. However, it is difficult to predict whether the chemical potential will eventually saturate to a constant based solely on few-body results.

APPLICABILITY TO THE HOMOGENEOUS SYSTEM

The calculations in this work are done for a trapped system. Our main results are reported in the harmonic trap length a_{ho} and the harmonic oscillator energy E_{ho} , which are the natural units in trapped systems. An important question is that, how does our results in a trap

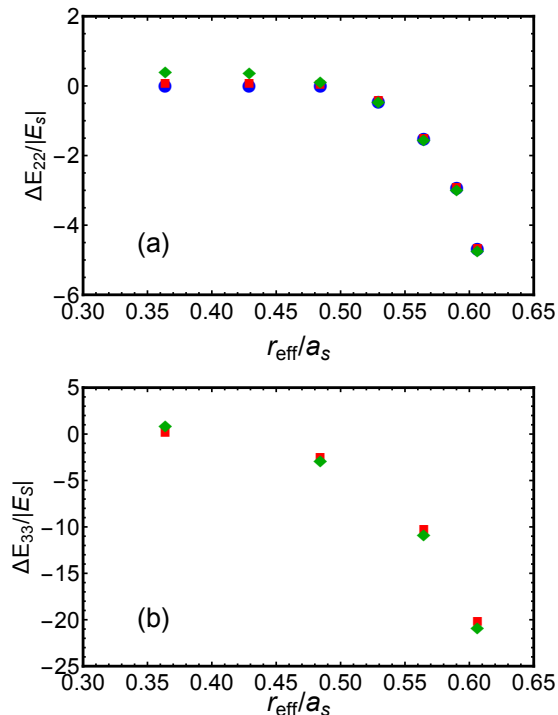


FIG. S2. (Color online) Panel (a) and (b) show the relative ground state energy for (2, 2) and (3, 3) systems subtracting the dimer energies, $\Delta E_{22} = E_{22} - 2E_{11}$ and $\Delta E_{33} = E_{33} - 3E_{11}$, as a function of effective range r_{eff} for type (i) potential. Lengths and energies are expressed in the unit of a_s and $|E_s| = \hbar^2/(ma_s^2)$, respectively. Blue circles [(2, 2) only], red squares, and green diamonds are for $a_s = 0.1a_{\text{ho}}$, $0.2a_{\text{ho}}$, and $0.5a_{\text{ho}}$, respectively.

connect to a homogeneous system.

For gas-like state, the average distance between like particles are of the order of a_{ho} . The energies are determined, to the leading order, by the trapping potential. The trap length is the most important length scale in this case.

For cluster state, the average distance between like particles are much smaller than a_{ho} . Because the size of the cluster state is an order of magnitude smaller than the a_{ho} , it is natural to expect that a_{ho} becomes an irrelevant length scale. In this case, the most relevant length scale is set by the s -wave scattering length a_s and the energy scale by the absolute value of zero-range binding energy $|E_s| = \hbar^2/(ma_s^2)$.

To examine if a_{ho} truly becomes irrelevant, we plot the relative ground state energies ΔE_{22} and ΔE_{33} calculated with different a_s/a_{ho} in Fig. S2 in terms of scattering unit a_s and $|E_s|$. We find the energies for cluster state roughly collapse. This indicates that for the parameter regime that we considered, the impact of the trapping potential to the energy of cluster state is small. Therefore, we expect that our condition for cluster formation and the

binding energy for cluster state should also apply to the homogeneous system.

EXPECTATION VALUES RELATED TO STRUCTURAL PROPERTIES

To gain more insights from the structural properties, we consider three expectation values calculated from the spherically symmetric radial density $P_1(r)$, the scaled distribution function between unlike pair $4\pi P_{12}(r)r^2$, and the scaled distribution function between like pair $4\pi P_{11}(r)r^2$. The expectation value $\langle r \rangle = 4\pi \int_0^\infty P_1(r)r^3 dr$ measures the overall extent of a single particle, while $\langle r_{12} \rangle = 4\pi \int_0^\infty P_{12}(r)r^3 dr$ and $\langle r_{11} \rangle = 4\pi \int_0^\infty P_{11}(r)r^3 dr$ measure the expected distance between unlike and like particles, respectively.

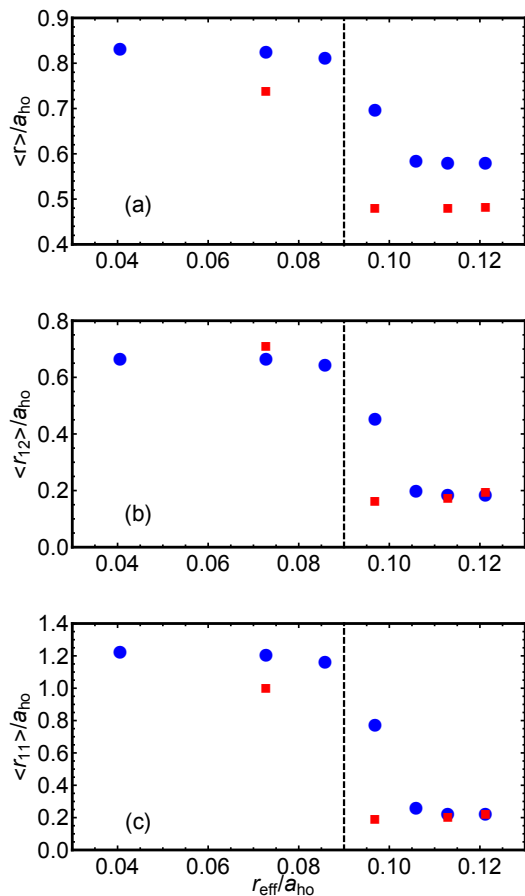


FIG. S3. (Color online) Panel (a), (b), and (c) show the expectation values $\langle r \rangle$, $\langle r_{12} \rangle$, and $\langle r_{11} \rangle$ as a function of effective range r_{eff} for $a_s = 0.2a_{\text{ho}}$. Blue circles and red squares are for (2, 2) and (3, 3) systems, respectively. Dashed vertical line $r_{\text{eff}} = 0.09a_{\text{ho}}$ marks the value of r_{eff} where clusters start to form.

Circles and squares in Fig. S3 show the three expectation values for (2, 2) and (3, 3) systems, respectively. In

both systems, a sudden decrease of all three expectation values occurs at around $r_{\text{eff}} = 0.09a_{\text{ho}}$, where the transition from gas-like state to cluster state occurs. This value is consistent with the transition point determined through bound state energy in the main text. Notably, $\langle r_{11} \rangle$ decreases by an order of magnitude as cluster forms.

ADDITIONAL DETAILS ON THE FESHBACH RESONANCE IN ^{40}K

We consider the Feshbach resonance between $|f, m_f\rangle = |9/2, -9/2\rangle$ and $|9/2, -5/2\rangle$ in ^{40}K [2]. We plot the relation between a_s and the magnetic field B in Fig. S4 according to the background scattering length $a_{\text{bg}} = 174a_0$, resonance peak $B_{\text{pk}} = 224.21 \pm 0.05\text{G}$ and width $w = 9.7 \pm 0.6\text{G}$, measured with high precision in Ref. [2]. Together with relation between r_{eff} and a_s discussed in the main text, we can determine the boundary between the cluster state and the gas-like state for this Feshbach resonance.

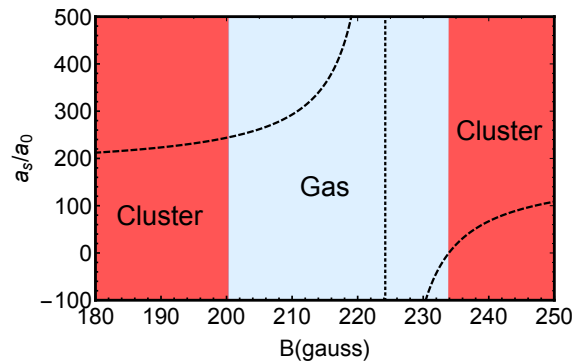


FIG. S4. (Color online) Dashed line shows a_s as a function of magnetic field B near the Feshbach resonance between $|f, m_f\rangle = |9/2, -9/2\rangle$ and $|9/2, -5/2\rangle$ of ^{40}K . Dotted vertical line marks the position of Feshbach resonance. The regime of cluster state is determined according to condition $0 < r_{\text{eff}} < 0.46a_s$.

-
- [1] D. S. Petrov, C. Salomon, and G. V. Shlyapnikov, Phys. Rev. Lett. **93**, 090404 (2004).
 - [2] C. A. Regal and D. S. Jin, Phys. Rev. Lett. **90**, 230404 (2003).